Fluorescence quantum yield of CdSe/ZnS nanocrystals investigated by correlated atomic-force and single-particle fluorescence microscopy

Y. Ebenstein, T. Mokari, and U. Banin[a)]
Institute of Chemistry and the Center for Nanoscience and Nanotechnology, The Hebrew University of Jerusalem, Jerusalem 91904, Israel

(Received 7 February 2002; accepted for publication 4 April 2002)

Correlated atomic-force and fluorescence microscopy are used to study single-particle versus ensemble fluorescence quantum yields (QY) of semiconductor nanocrystals by measuring a simultaneous map of the topography and the single-particle fluorescence. CdSe/ZnS nanocrystal quantum dots and quantum rods with high QY were investigated. A significant portion of dark particles is detected. Comparison with the ensemble solution QY shows that samples with higher QY have a larger fraction of bright particles accompanied by an increased single-particle QY. Saturated emission from single nanocrystals could not be detected because of particle darkening under high-power excitation. © *2002 American Institute of Physics.* [DOI: 10.1063/1.1482785]

The emission tunability via the quantum-confinement effect of semiconductor nanocrystals renders them useful as chromophores for a wide range of applications from biological fluorescent markers[1,2] to light-emitting diodes[3,4] and as laser materials.[5,6] Fluorescence quantum yields (QYs) in the range of 10%–50% can be achieved and used advantageously in such applications, covering the visible to the near-IR spectral range by control of particle composition and size.[7–10] The high QY is obtained by growing a shell of a high-band-gap semiconductor on the core, a rather complex although well-studied process. In this process different sources of inhomogeneity, such as variations in size of both core and shell and incomplete shell growth, give rise to differences between particles in a given preparation. Here, we use a correlated atomic-force and fluorescence microscopy method to investigate whether the quantum yield of such samples is limited by single-particle properties or whether it arises from a fraction of bright emitters. Such information is important for the further understanding of nanocrystal photophysical properties as well as for their further development as useful and reliable bright chromophores. This is of particular relevance to future applications utilizing fluorescence of single particles, for example, in DNA sequencing.[1]

The importance of single-particle fluorescence studies for understanding the photophysics of semiconductor nanocrystals has been demonstrated in numerous studies, revealing phenomena such as fluorescence blinking and spectral wandering.[11–17] However, these single-particle studies have been mostly limited to probing the optical characteristics and are, therefore, blind to dark particles. Buratto and co-workers previously measured the fluorescence and shear-force images for porous-silicon samples,[18] and although the measurements were not taken in a correlated fashion, they could conclude that the ensemble QYs of 1%–10% was attributed to a small fraction of bright particles. We address the issue of fluorescence QY in single CdSe quantum dots and quantum rods by determining the ratio of emitting versus the total number of particles in a given sample. Unlike previous studies, we utilize a method of simultaneous, correlated atomic-force microscopy (AFM) and scanning fluorescence microscopy to determine the number of emitting particles within an ensemble. This directly detects whether a specific particle is bright or dark. Cases where more than one particle or particle aggregates are detected by AFM can be ignored, and thus the method enables reliable analysis of the correlated single-particle fluorescence image. Furthermore, using the AFM probe, it is possible to determine the particle size. These data are compared to the QY measured in the ensemble solution.

We investigated CdSe nanocrystals, a highly synthetically developed model system for the investigation of semiconductor nanocrystal photophysics. Four different samples of CdSe nanocrystals with different QYs and emission in the range of 575–600 nm (see Table I for a summary of the sample properties and the QYs) were studied. Samples A–C are nearly spherical CdSe/ZnS core/shell nanocrystal quantum dots (QDs) prepared by the established methods of colloidal nanocrystal synthesis utilizing high-temperature pyrolysis of organometallic precursors in coordinating solvents.[8,9] Samples B and C are capped by trioctylphosphine oxide (TOPO), and the difference in their QYs reflects variation of synthesis conditions in these two cases. Sample A is capped by a mixture of TOPO and hexadecyl amine (HDA), a combination that yields the highest QY. For sample

TABLE I. Summary of the results for the four samples studied. Samples A–C are spherical CdSe/ZnS nanocrystals, with average core diameters of 3, 3, and 3.5 nm, respectively, with a nominal ZnS shell thickness of ~1.5 ML. Sample D is a CdSe/ZnS quantum-rod sample with total average diameter of 4 nm and average length of 25 nm.

Sample	QY in solution	Bright/total particles		Average QY for emitting particles
A	48%	38/75	51%	94%
B	32%	84/194	43%	74%
C	18%	45/135	33%	55%
D	12%	35/110	32%	37%

a)Author to whom correspondence should be addressed; electronic mail: banin@chem.ch.huji.ac.il

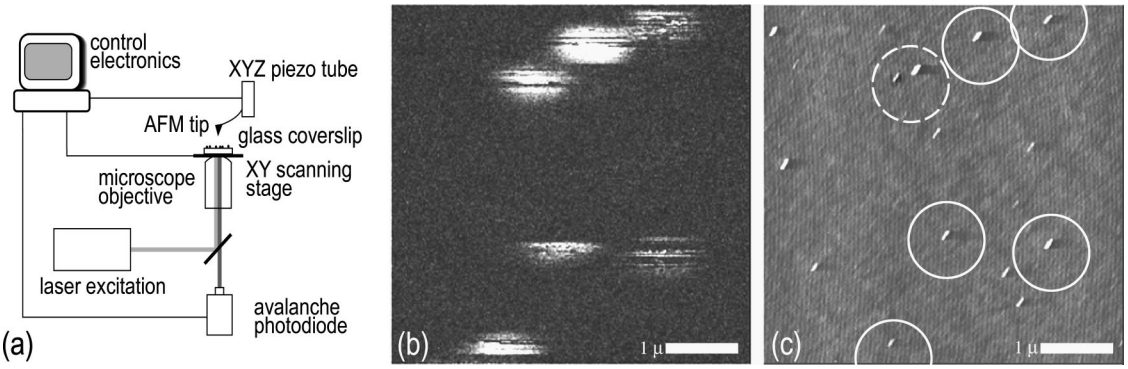

FIG. 1. (A) Schematic of the experimental setup for correlated AFM and single-particle fluorescence measurements. (B) and (C) are correlated fluorescence (B) and height (C) images measured for sample C. The circles mark bright particles, while the dashed circle indicates a case where two particles correlate with the same fluorescence spot. The elongated appearance of the particles in the AFM image is due to a tip artifact.

D we used the recently developed shape control mechanism[19] to prepare a CdSe/ZnS quantum-rod sample with average dimensions of 25×4 nm.[6] We specifically chose these four samples as they cover a wide range of solution QYs from medium (12%) to high ($\sim$50%). For the single-nanocrystal measurements, an extremely dilute solution of each sample was spin cast on a glass coverslip. Special effort was required in preparing suitable substrates that have no fluorescence background while maintaining surface flatness required for the AFM studies.[20]

The setup for simultaneous AFM topography and fluorescence measurements is shown schematically in Fig. 1(a). A commercial AFM (DI bioscope) was mounted on an inverted optical microscope (Zeiss axiovert). The AFM visible laser diode was replaced by a near-IR laser diode to avoid optical interference in the fluorescence image. The samples were excited by an Ar-ion laser using the 514.5 nm line that was circularly polarized and focused to a diffraction-limited spot through a high-numerical-aperture (NA=1.4) oil immersion objective. As a first step towards correlated measurement of the sample, the AFM tip is scanned over the excitation spot. The scattered laser light is collected with the same objective and directed to an avalanche photodiode. A distinct signal maxima is revealed as the tip passes over the laser spot allowing for the precise positioning of the AFM tip in the center of the illumination spot. After alignment of the tip, a piezoelectric stage (Nanonics flatscanner) located between the microscope objective and the AFM tip, raster scans the substrate over the excitation spot and both fluorescence and height signals are collected pixel by pixel to create correlated simultaneous photon and height images of the same area.

Figure 1(b) (fluorescence intensity) and Fig. 1(c) (AFM height, in tapping mode) present a typical correlated scan for sample C. The lateral sizes of the features in the height scan are significantly smaller than the corresponding diffraction-limited fluorescence spots, but are larger than the $\sim$4 nm dimension of the nanocrystals due to the tip convolution effect. The height does not involve convolution and, therefore, provides a more accurate measure of the particle size. The fluorescence spots exhibit streaks corresponding to the on–off blinking behavior of the particle luminescence.[11] In the correlated images we can identify bright particles (marked by circles) and dark particles. The dashed circle presents a case where two particles correlate with the same fluorescence spot. Therefore, correlated scans provide a means to screen the optical data to cases where strictly single particles are observed. We note that the possibility of perturbation of the fluorescence by the tip will not have a significant effect on the results. This is so because the emission is detected in the far field over a large range of tip–particle distances, while the perturbation of the fluorescence by the tip is a near-field process active only at short tip–particle distances.

Similar scans were collected for statistically significant numbers of particles for each of the samples. The use of circular polarized excitation eliminates orientational effects in the particle absorption. To reduce the possibility that potentially bright particles were in a dark period during a scan, low-light powers were used (0.15 kW/cm^2) reducing the blinking, and repetitive scans of the same area were performed. Particles were considered as bright if they exhibited even very partial fluorescence above the background level ($>$1 kcps) in any of their images. This is a reasonable method of analysis as the blinking process is not an important phenomenon in the low-light-level regime used in ensemble solution QY measurements. Few cases were identified where a fluorescence spot did not have a corresponding AFM feature and were not taken into account. Cases where more than one particle occupied the region of the fluorescence spot were also ignored, but with the high dilution used in our samples these were not common.

The ratio between the bright and total number of particles for the four samples is summarized in Table I. Using this ratio and the solution QY, a value for the average single-particle QY can be easily extracted. Both the ratio and the single-particle QY increase for samples with the higher solution QY, as is presented in Fig. 2. The rod-shaped sample (D), follows the same trend. In molecules one may expect a uniform average single-molecule QY, while for the nanocrystals, variation in composition, defects, and surface imperfections lead to a distribution of single-particle QYs. A nearly unity single-particle QY inferred for the brightest sample (A), implies that the solution QY is still limited by the presence of a fraction of dark particles, suggesting that further improvements can be achieved by modifying the synthesis.

We also tried to estimate the single-particle QY from saturation and lifetime measurements as was previously reported for porous-silicon particles.[18] The inset of Fig. 3

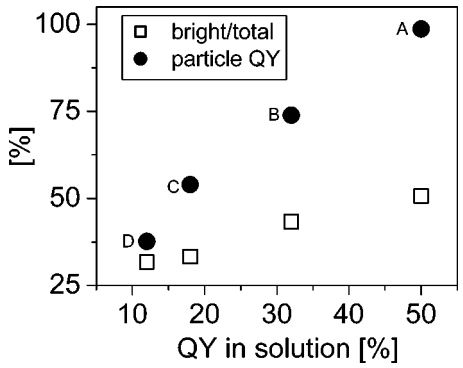

FIG. 2. Ratio of bright/total particles (open squares), and the average single-particle QY (filled circles) vs solution QY for the four samples.

shows the fluorescence decay of sample B in toluene solution measured using 410 nm excitation from a 50 ps laser diode and a multi-channel-plate photomultiplier tube with time-correlated single-photon counting. The decay is clearly non-exponential and was fit with the Williams–Watts stretched exponential function.[21] The fit yielded an average lifetime of ~25 ns. With this lifetime an upper limit for the measured saturation emission rate of a single particle can be estimated as ~2 Mcps, taking into account the 0.045 detection efficiency of our system. However, particles darken at considerably lower emission rates, as can be seen in Fig. 3, showing the emission count rate versus increasing excitation power. Typically, particles did not exceed count rates of 300 kHz, far from the expected saturation value. This result agrees with the observation that the probability for long on times decreased upon increasing the excitation intensity.[16]

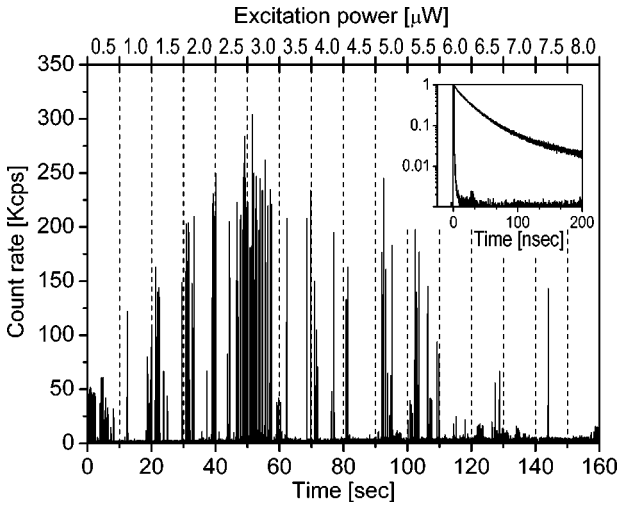

FIG. 3. Emission count rate as a function of increasing excitation power for a single particle from sample B. Excitation power, indicated in the top axis, was increased in steps of 0.5 μW every 10 s. Between each interval, the excitation was blocked for 10 s to allow for the recovery of the particle fluorescence (these intervals are not shown). The inset shows the fluorescence decay trace for sample B in solution along with the best fit to the stretched exponential function. A trace representing the excitation pulse is presented.

In conclusion, only a fraction of the nanocrystals are bright. Unlike in molecules, the measured QY of nanocrystals varies between different particles. The samples with higher solution QY not only have a higher percentage of bright particles, but also a larger single-particle QY, reflecting improved intrinsic particle fluorescence properties.

This work was supported by the Israel Science Foundation (Grant No. 99/00-12.5).

[1] M. P. Bruchez, M. Moronne, P. Gin, S. Weiss, and A. P. Alivisatos, Science **281**, 2013 (1998).
[2] W. C. W. Chan and S. Nie, Science **281**, 2016 (1998).
[3] V. L. Colvin, M. C. Schlamp, and A. P. Alivisatos, Nature (London) **370**, 354 (1994).
[4] N. Tessler, V. Medvedev, M. Kazes, S. H. Kan, and U. Banin, Science **295**, 1506 (2002).
[5] V. I. Klimov, A. A. Mikhailovsky, S. Xu, J. A. Hollingsworth, C. A. Leatherdale, H. J. Eisler, and M. G. Bawendi, Science **290**, 314 (2000).
[6] M. Kazes, D. Y. Lewis, Y. Ebenstein, T. Mokari, and U. Banin, Adv. Mater. **14**, 317 (2002).
[7] M. A. Hines and P. J. Guyot-Sionnest, J. Phys. Chem. **100**, 468 (1996).
[8] B. O. Dabbousi, J. Rodriguez-Viejo, F. V. Mikulec, J. R. Heine, H. Mattoussi, R. Ober, K. F. Jensen, and M. G. Bawendi, J. Phys. Chem. B **101**, 9463 (1997).
[9] D. V. Talapin, A. L. Rogach, A. Kornowski, M. Haase, and H. Weller, Nano Lett. **1**, 207 (2001).
[10] Y. W. Cao and U. Banin, Angew. Chem. Int. Ed. Engl. **38**, 3692 (1999).
[11] M. Nirmal, B. O. Dabbousi, M. G. Bawendi, J. J. Macklin, and L. E. Brus, Nature (London) **383**, 802 (1996).
[12] U. Banin, M. P. Bruchez, A. P. Alivisatos, T. J. Ha, S. Weiss, and D. S. Chemla, J. Chem. Phys. **110**, 1195 (1999).
[13] M. Kuno, D. P. Fromm, H. F. Hamman, A. Gallaghar, and D. J. Nesbitt, J. Chem. Phys. **112**, 3117 (2000).
[14] R. G. Neuhauser, K. T. Shimizu, W. K. Woo, S. A. Empedocles, and M. G. Bawendi, Phys. Rev. Lett. **85**, 3301 (2000).
[15] M. Kuno, D. P. Fromm, A. Gallegher, D. J. Nesbitt, O. I. Micic, and A. J. Nozik, Nano Lett. **1**, 557 (2001).
[16] K. T. Shimizu, R. G. Neuhauser, C. A. Leatherdale, S. A. Empedocles, W. K. Woo, and M. G. Bawendi, Phys. Rev. B **63**, 205316 (2001).
[17] F. Koberling, A. Mews, and T. Basche, Adv. Mater. **13**, 672 (2001).
[18] G. M. Credo, M. D. Mason, and S. K. Buratto, Appl. Phys. Lett. **74**, 1978 (1999).
[19] X. G. Peng, L. Manna, W. D. Yang, J. Wickham, E. Scher, A. Kadavanich, and A. P. Alivisatos, Nature (London) **404**, 59 (2000).
[20] Glass coverslips were baked at 500 °C for 2 h and then immersed for 15 min in RCA solution (1:1:4, 30% H_2O_2: 30% NH_4OH: high-purity water) at 85 °C, washed with high-purity water, and dried with N_2 flow.
[21] G. Williams and D. C. Watts, Trans. Faraday Soc. **66**, 80 (1970).